Bergische Universität Wuppertal

Fachbereich Mathematik und Naturwissenschaften

Lehrstuhl für Angewandte Mathematik
und Numerische Mathematik

Lehrstuhl für Optimierung und Approximation

Preprint BUW-AMNA-OPAP 10/19

Sebastian Schöps, Andreas Bartel, and Herbert De Gersem

Multirate Time Integration of Field/Circuit Coupled Problems by Schur Complements

October 2010

http://www.math.uni-wuppertal.de

Multirate Time Integration of Field/Circuit Coupled Problems by Schur Complements

Sebastian Schöps[1,2], Andreas Bartel[1], and Herbert De Gersem[2]

Abstract When using distributed magnetoquasistatic field models as additional elements in electric circuit simulation, the field equations contribute with large symmetric linear systems that have to be solved. The naive coupling and solving (using direct solvers) is not always efficient, since the electric circuit is coupled only via coils, which are often represented only by a small subset of the unknowns. We revisit the Schur complement approach, give a physical interpretation and show that a heuristics for bypassing Newton iterations allow for efficient multirate time-integration for the field/circuit coupled model.

1 Introduction

Circuit simulators assemble the underlying equations element-wise, usually by modified nodal analysis (MNA). Each element contributes with an element stamp that describes the current/voltage relation and possibly internal equations. This results in a system of Differential Algebraic Equations (DAEs). In our case of the field/circuit problem, parts of this system stem from Maxwell's equations.

In the next section, we summarize the mathematical model for coupled electric circuits with maqnetoquasistatic (MQS) field devices. Our point of view stresses the usual assembly via stamping during time discretization. In the following section, we introduce a Schur complement approach for the MQS stamp, cf. [**?**, **?**]. The fourth section deals with the corresponding computational cost. Then, in section five, a bypassing technique of the Jacobian, similar to simplified Newton, and the bypassing of the right-hand-side are interpreted and employed as a multirate time-integration scheme. Also bypassing is a common technique in classical circuit simulation, but here the energy balances of field and circuit are taken into account. The paper is completed by numerical results and conclusions.

Bergische Universität Wuppertal {schoeps,bartel}@math.uni-wuppertal.de · Katholieke Universiteit Leuven Herbert.DeGersem@kuleuven-kortrijk.be

2 Mathematical Model Description and Time Discretization

Common circuit simulators use MNA to assemble the circuit equations element-wise. Each element contributes with differential and algebraic relations to the underlying DAE, [**?**]. To the list of basic elements, the magnetoquasistatic (MQS) device is added (with subscript M), which allows the coupling to field effects while still using MNA. For each element we have a model $\mathbf{f}_e$ consisting of current balances for the network nodes (except ground) and additional constitutive relations for non-current defining elements, which gives

$$\mathbf{f}(\dot{\mathbf{y}},\mathbf{y},t) := \sum_e \mathbf{Q}_e \mathbf{f}_e\left(\frac{\mathrm{d}}{\mathrm{d}t}\mathbf{y}_e,\mathbf{y}_e,t\right) + \mathbf{Q}_M \mathbf{f}_M\left(\frac{\mathrm{d}}{\mathrm{d}t}\mathbf{y}_M,\mathbf{y}_M\right) = 0 \tag{1}$$

using for element e: local variables $\mathbf{y}_e$ and generalized topology matrices $\mathbf{Q}_e$ that map local to global variables, such that holds $\mathbf{y}_e = \mathbf{Q}_e^\top \mathbf{y}$. The global unknowns $\mathbf{y}$ consist of the node potentials, whose differences define the respective voltage drop $\mathbf{v}_e$ at each element, and of several currents in particular the currents through MQS devices $\mathbf{i}_M$, [**?**]. All currents contribute to the balances required by Kirchhoff's Current Law (KCL), which is included in (**??**).

The field distribution of the MQS device is described in terms of the degrees of freedom of the discretized magnetic vector potential (MVP) $\widehat{\mathbf{a}} = \widehat{\mathbf{a}}(t)$, e.g. by the finite integration technique (FIT) or the finite element method (FEM):

$$\mathbf{M}\frac{\mathrm{d}}{\mathrm{d}t}\widehat{\mathbf{a}} + \mathbf{K}(\widehat{\mathbf{a}})\widehat{\mathbf{a}} = \mathbf{X}\mathbf{i}_M, \tag{2a}$$

$$\mathbf{X}^\top \frac{\mathrm{d}}{\mathrm{d}t}\widehat{\mathbf{a}} = \mathbf{v}_M - \mathbf{R}\mathbf{i}_M. \tag{2b}$$

Equation (**??**) stems from the continuous curl-curl equation, where $\mathbf{M}$ and $\mathbf{K}(\widehat{\mathbf{a}})$ denote the singular conductivity matrix and the curl-curl matrix with the nonlinear reluctivity $\nu(\widehat{\mathbf{a}})$ employed. $\mathbf{K}(\widehat{\mathbf{a}})$ includes gauging, boundary and initial conditions, [**?**], such that a regular matrix pencil is obtained. The columns of the coupling matrix $\mathbf{X} = [\mathbf{X}_1,\ldots,\mathbf{X}_p]$ distribute the branch currents $\mathbf{i}_M$ on the spatial grid, [**?**].

The second equation is the coupling equation: it relates the branch voltage $\mathbf{v}_M$ to the MVP and to the branch current using linear DC resistance $\mathbf{R}$. All common conductor types (solid, stranded and foil conductors) can be realized in (**??**) by the structure of the conductivity matrix, [**?**]. Summing up, the field model $\mathbf{f}_M$ in (**??**) reads:

$$\mathbf{f}_M\left(\frac{\mathrm{d}}{\mathrm{d}t}\mathbf{y}_M,\mathbf{y}_M\right) := \begin{bmatrix} \mathbf{i}_M \\ \mathbf{X}^\top \frac{\mathrm{d}}{\mathrm{d}t}\widehat{\mathbf{a}} - \mathbf{v}_M + \mathbf{R}\mathbf{i}_M \\ \mathbf{M}\frac{\mathrm{d}}{\mathrm{d}t}\widehat{\mathbf{a}} + \mathbf{K}(\widehat{\mathbf{a}})\widehat{\mathbf{a}} - \mathbf{X}\mathbf{i}_M \end{bmatrix}, \quad \text{where } \mathbf{y}_M = \begin{bmatrix} \mathbf{i}_M \\ \mathbf{v}_M \\ \widehat{\mathbf{a}} \end{bmatrix}, \tag{3}$$

where the first row contains the contribution to the KCL and the last row represent the curl-curl equation (**??**).

Typically, circuit simulators use BDF schemes for time discretization. This gives for constant step size h a nonlinear system at each discrete time t_n for $\mathbf{y}_n \approx \mathbf{y}(t_n)$, [**?**]:

$$\mathbf{f}\left(\frac{1}{h}\rho\mathbf{y}_n,\mathbf{y}_n,t_n\right)=0 \quad \text{with} \quad \frac{1}{h}\rho\mathbf{y}_n := \frac{1}{h}\sum_{i=0}^{k}\alpha_i\mathbf{y}_{n-i}\approx\dot{\mathbf{y}}_n$$

using coefficients α_i (k-th order BDF). As usually Newton-Raphson is applied:

$$\mathbf{J}_n^{(i)}\mathbf{y}_n^{(i+1)}=-\mathbf{f}_n^{(i)}+\mathbf{J}_n^{(i)}\mathbf{y}_n^{(i)} \quad \text{with} \quad \mathbf{J}_n^{(i)} := \frac{\partial\mathbf{f}}{\partial\mathbf{y}_n}\left(\frac{1}{h}\rho\mathbf{y}_n^{(\mathrm{i})},\mathbf{y}_n^{(\mathrm{i})},t_n\right) \qquad (4)$$
$$\mathbf{f}_n^{(i)} := \left(\frac{1}{h}\rho\mathbf{y}_n^{(\mathrm{i})},\mathbf{y}_n^{(\mathrm{i})},t_n\right).$$

Due to the structure of (**??**), the assembly of the Newton system (**??**) is performed by a cycle over all circuit elements (which can be organized in parallel), such that

$$\mathbf{J}_n^{(i)} := \sum_{e,M}\mathbf{Q}_e\mathbf{J}_e^{(i)}\mathbf{Q}_e^\top \text{ with } \mathbf{J}_e^{(i)} := \frac{\alpha_0}{h}\frac{\partial\mathbf{f}_e^{(i)}}{\partial\dot{\mathbf{y}}_e}+\frac{\partial\mathbf{f}_e^{(i)}}{\partial\mathbf{y}_e},\ \mathbf{f}_e^{(i)} := \mathbf{f}_e\left(\frac{1}{h}\rho\mathbf{y}_e^{(i)},\mathbf{y}_e^{(i)},t_n\right) \qquad (5)$$

suppressing the time index n. This resembles the element-wise assembly in FEM. Each contribution ('*stamp*'), $\mathbf{J}_e^{(i)}$, $\mathbf{f}_e^{(i)}$, consists of inner and external variables, i.e., variables used only inside the particular element and variables related to other elements by the simulator, [**?**].

In the following we want to speed up solving the Newton system by elimination of the MVP $\widehat{\mathbf{a}}$. Therefore we work out the MQS stamp and revisit the Schur complement next.

3 MQS Stamp and Schur Complement

For the MQS model (**??**) in terms of $\mathbf{y}_M^\top=(\mathbf{i}_M^\top,\mathbf{v}_M^\top,\widehat{\mathbf{a}}^\top)$, we obtain the following Jacobian stamp (for BDF time discretization):

$$\mathbf{J}_M^{(i)} := \begin{bmatrix}\mathbf{I} & 0 & 0\\ \mathbf{R} & -\mathbf{I} & \frac{\alpha_0}{h}\mathbf{X}^\top\\ -\mathbf{X} & 0 & \mathbf{K}_h^{(i)}\end{bmatrix} \qquad \text{with} \quad \mathbf{K}_h^{(i)} := \underbrace{\left.\frac{\mathrm{d}\mathbf{K}(\widehat{\mathbf{a}})}{\mathrm{d}\widehat{\mathbf{a}}}\right|_{\widehat{\mathbf{a}}=\widehat{\mathbf{a}}^{(i)}}}_{=:\mathbf{k}_a(\widehat{\mathbf{a}}^{(i)})}+\frac{\alpha_0}{h}\mathbf{M} \qquad (6)$$

and differential reluctivity matrix $\mathbf{k}_a(\widehat{\mathbf{a}}^{(i)})$. The function-evaluation stamp reads:

$$\mathbf{f}_M^{(i)} := \begin{bmatrix}\mathbf{I} & 0 & 0\\ \mathbf{R} & -\mathbf{I} & 0\\ -\mathbf{X} & 0 & \mathbf{K}(\widehat{\mathbf{a}}^{(i)})\end{bmatrix}\mathbf{y}_M^{(i)}+\begin{bmatrix}0\\ \mathbf{X}^\top\\ \mathbf{M}\end{bmatrix}\frac{1}{h}\rho\widehat{\mathbf{a}}^{(i)}.$$

and the right-hand side contribution is given by:

$$\mathbf{r}_M^{(i)} := -\mathbf{f}_M^{(i)}+\mathbf{J}_M^{(i)}\mathbf{y}_M^{(i)} = \frac{1}{h}\begin{bmatrix}0\\ \mathbf{X}^\top\\ \mathbf{M}\end{bmatrix}\left(\alpha_0\widehat{\mathbf{a}}^{(i)}-\rho\widehat{\mathbf{a}}^{(i)}\right)+\begin{bmatrix}0\\ 0\\ \mathbf{k}_a(\widehat{\mathbf{a}}^{(i)})-\mathbf{K}(\widehat{\mathbf{a}}^{(i)})\end{bmatrix}\widehat{\mathbf{a}}^{(i)}. \qquad (7)$$

For the MQS devices, only the current/voltage relation of the series connection of a (nonlinear) inductor and a resistor needs to be unveiled to the host circuit simulator.

But the inner variables $\widehat{\mathbf{a}}$ is not used outside the MQS stamp, it can be eliminated from the Newton system by the well-known Schur complement, that is, to indeed reduce the element stamp. – This is especially beneficial for all kinds elements with rather large stamps, e.g. semiconductors, [**?**], or MQS device, [**?**], since more compact stamps are obtained, which fit better into the overall framework. – Removing $\widehat{\mathbf{a}}$ yields a reduced stamp in terms of $\widetilde{\mathbf{y}}_M^\top = (\mathbf{i}_M^\top, \mathbf{v}_M^\top)$. The reduced Jacobian reads

$$\widetilde{\mathbf{J}}_M^{(i)} := \begin{bmatrix} \mathbf{I} & 0 \\ \mathbf{R} + \frac{\alpha_0}{h}\mathbf{L}_h^{(i)} & -\mathbf{I} \end{bmatrix} = \begin{bmatrix} \mathbf{I} & 0 & 0 \\ 0 & \mathbf{I} & -\frac{\alpha_0}{h}\mathbf{X}^\top \left(\mathbf{K}_h^{(i)}\right)^{-1} \end{bmatrix} \mathbf{J}_M^{(i)} \begin{bmatrix} \mathbf{I} & 0 \\ 0 & \mathbf{I} \\ 0 & 0 \end{bmatrix} \tag{8}$$

with generalized inductance matrix

$$\mathbf{L}_h^{(i)} := \mathbf{X}^\top \left(\mathbf{K}_h^{(i)}\right)^{-1} \mathbf{X} \tag{9}$$

using $\mathbf{K}_h^{(i)}$ from (**??**) and corresponding reduced right-hand side contribution:

$$\widetilde{\mathbf{r}}_M^{(i)} = \begin{bmatrix} 0 \\ \widetilde{\mathbf{r}}_{M,v}^{(i)} \end{bmatrix} \quad \text{where} \quad \widetilde{\mathbf{r}}_{M,v}^{(i)} = \frac{1}{h}\mathbf{X}^\top \left(\mathbf{I} - \frac{\alpha_0}{h}\left(\mathbf{K}_h^{(i)}\right)^{-1}\mathbf{M}\right)(\alpha_0 \widehat{\mathbf{a}}^{(i)} - \rho\, \widehat{\mathbf{a}}^{(i)}) - \frac{\alpha_0}{h}\mathbf{X}^\top \left(\mathbf{K}_h^{(i)}\right)^{-1} \left(\mathbf{k}_a(\widehat{\mathbf{a}}^{(i)}) - \mathbf{K}(\widehat{\mathbf{a}}^{(i)})\right) \widehat{\mathbf{a}}^{(i)}.$$

We notice that the MVP needs still to be computed to evaluate the reduced right-hand side (and the nonlinear material curve). Equation (**??**) corresponds the common inductance extraction approach, [**?**], but in addition the Schur complement takes eddy current effects into account (due to the conductance matrix). – Moreover, the dimension of the reduced stamp is independent of the space discretization of the field problem. Thus the spatial mesh can be refined and coarsened during the time-integration without restarting the host-simulator. Nevertheless, the reduction comes with additional cost.

4 Computational Cost for Schur Complement (Direct Solver)

For the Schur complement in the Newton iteration $i+1$, we need to compute $\mathbf{L}_h^{(i)}$. Applying a direct solver, the matrix $\mathbf{K}_h^{(i)}$ has to be factorized (one LU decomposition) and forward/backward substitutions for the vector potentials in each branch:

$$\mathbf{K}_h^{(i)} \widehat{\mathbf{a}}_{M,j}^{(i)} = \mathbf{X}_j \qquad (\text{for } j = 1, \ldots, p), \quad \text{s.t.} \quad \mathbf{L}_h^{(i)} = \mathbf{X}^\top \widehat{\mathbf{a}}_M^{(i)} \tag{10}$$

by sparse inner products. Also, the MVP for the right-hand-side voltage must be computed. To this end, we project onto the MVP defining equation inside the Newton iteration (derived from Jacobian (**??**) and right-hand side (**??**)):

$$\mathbf{K}_h^{(i)}\widehat{\mathbf{a}}^{(i+1)} = \mathbf{r}_{M,a}^{(i)} + \mathbf{X}\mathbf{i}_M^{(i+1)}, \quad \mathbf{r}_{M,a}^{(i)} := \frac{1}{h}\mathbf{M}\left(\alpha_0\widehat{\mathbf{a}}^{(i)} - \rho\widehat{\mathbf{a}}^{(i)}\right) + \left(\mathbf{k}_a(\widehat{\mathbf{a}}^{(i)}) - \mathbf{K}(\widehat{\mathbf{a}}^{(i)})\right)\widehat{\mathbf{a}}^{(i)}.$$

Thus we compute the remaining term $\widehat{\mathbf{a}}_V^{(i)}$ by forward/backward substitutions from:

$$\mathbf{K}_h^{(i)}\widehat{\mathbf{a}}_V^{(i)} = \mathbf{r}_{M,a}^{(i)}, \tag{11}$$

and obtain for the MVP

$$\widehat{\mathbf{a}}^{(i+1)} = \widehat{\mathbf{a}}_V^{(i)} + \widehat{\mathbf{a}}_M^{(i)}\mathbf{i}_M^{(i+1)}.$$

Moreover, we obtain for the reduced right-hand side the simplification:

$$\widetilde{\mathbf{r}}_{M,v}^{(i)} = \frac{1}{h}\mathbf{X}^\top\left(\alpha_0\widehat{\mathbf{a}}^{(i)} - \rho\,\widehat{\mathbf{a}}^{(i)} - \widehat{\mathbf{a}}_V^{(i)}\right).$$

Thus one LU-decomposition and $p+1$ forward/backward substitutions are necessary for the Schur complement. The choice of solver for the Schur complement is independent of the solver used in circuit host simulator. So, for example an iterative method such as block-PCG could be used. Such a procedure should support multiple right-hand-sides, as [**?**], for efficiency. A further advantage of iterative methods applied to 3D problems is the *weak gauging* introduced by the iterative solver, [**?**], such that further gauging, as employed here, becomes unnecessary.

5 Bypassing as Multirate Time Integration

The generalized inductance matrix depends on the saturation (BH-curve), but this effect is rather slow compared to other time rates of the electric circuit, e.g. the switching frequency of transistors, [**?**]. Saturation depends on the supplied energy

$$\mathbf{E}(t_n) = \int_0^{t_n} \mathbf{i}_M(s)\mathbf{v}_M(s)\mathrm{d}s \tag{12}$$

and thus the relevant time scale of the nonlinearity is given by the integral above, even if the applied voltage is a much faster signal. We approximate (**??**) by

$$\mathbf{E}_n \approx h\left(\sum_{j=0}^{n-1}\mathbf{i}_M(t_j)\mathbf{v}_M(t_j) + \mathbf{i}_M^{(i)}\mathbf{v}_M^{(i)}\right)$$

and compare this to the energy saved in the magnetic field. Consequently, updates of this matrix are often superfluous and whenever the material behaves (nearly) linearly, then only one forward/backward substitution for the right-hand-side per iteration is necessary. This allows an interpretation as a simplified Newton algorithm, where the Jacobian (**??**) is frozen across several iterations and possibly several time steps if the (relative) change of energy does not exceed a threshold and if the reluctivity is (nearly) constant.

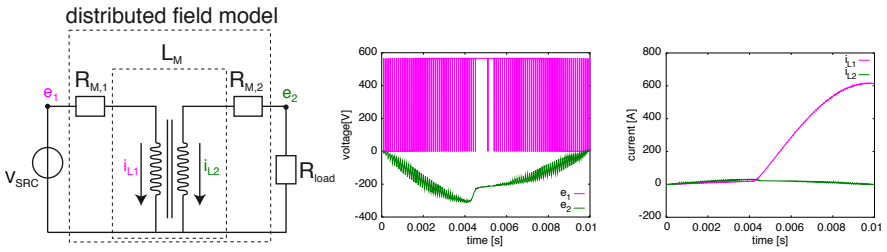

(a) Transformer circuit. (b) Applied nodal potentials. (c) Currents through coils.

Fig. 1: Transformer: setup and reference solution.

Furthermore, if the material is rather linear the right-hand-side evaluation can be bypassed as well: then the vector potential needs no update and the distributed field problem is decoupled from the circuit, where it is represented by an inductance matrix, similarly to the co-simulation approach, [**?**].

0) compute $\widehat{\mathbf{a}}^{(i)}$

1) approximate the energy $\mathbf{E}_n^{(i)}$

2) **if** $||\mathbf{E}_n^{(i)} - \mathbf{E}_0|| > tol$

then evaluate material curve $\nu^{(i)} := \nu(\widehat{\mathbf{a}}^{(i)})$

2a) **if** $||\nu^{(i)} - \nu^{(i-1)}|| > tol$

then compute $\mathbf{L}_h^{(i)}$ and $\mathbf{v}_M^{(i)}$

else bypass matrix update $\mathbf{L}_h^{(i)} := \mathbf{L}_h^{(i-1)}$ and $\mathbf{v}_M^{(i)} := \mathbf{v}_M^{(i-1)}$

else bypass material update $\nu^{(i)} := \nu^{(i-1)}$ and $\mathbf{L}_h^{(i)} := \mathbf{L}_h^{(i-1)}$, $\mathbf{v}_M^{(i)} := \mathbf{v}_M^{(i-1)}$

3) return to host simulator.

This algorithm unburdens the host simulator from solving unnecessarily large system of equations, while still having a suitable Jacobian information at hand. The drawback are additional Newton iterations due to the inferior convergence of simplified Newton, but solving a sequence of reduced system. If eddy currents included into the model, the inductance matrix $\mathbf{L}_h = \mathbf{L}(\widehat{\mathbf{a}}, h)$ depends on the time step step size h and therefore the matrix must be recomputed or interpolated for any change of h.

6 Computational Results

All presented methods, the standard Newton without Schur complement, and the ones using the Schur approach, i.e., simplified and bypassed Newton, have been implemented in the Framework of the CoMSON DP. In Fig. **??** a simple example circuit is shown, where a pulse width modulated (PWM) voltage source is connected to the primary side of a transformer. The PWM is switching at 20kHz, Fig, **??**. The secondary side is connected by a resistor. This transformer has a highly nonlinear behavior that is simulated until its saturation phase is reached, Fig. **??**.

	decompositions	forward/backward substitutions	stamp evaluations	time
full Newton	23371	27936	27936	20h
simplified Newton	2531	36460	31398	1h
bypassed Newton	450	3171	20449	25min

Table 1: Transformer: computational costs.

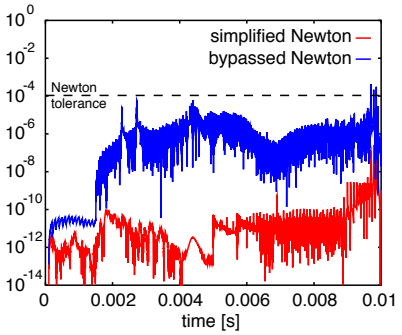

(a) Relative errors with respect to the reference solution obtained by full Newton-Raphson

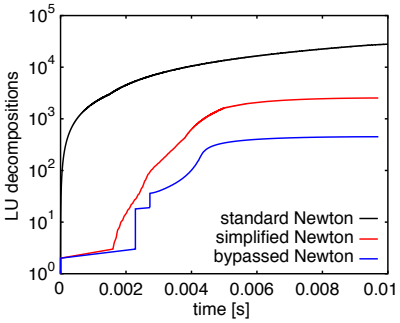

(b) Number of LU decompositions, full Newton requires one decomposition per iteration.

Fig. 2: Transformer: reference solution, errors and decompositions.

In the beginning of the start-up phase, $t \leq 0.03s$, both, the simplified and bypassed Newton methods detect the linearity in the material and skip the superfluous evaluations and the LU decompositions, Fig. **??**, although the applied voltages and currents are fast switching due to the PWM. The standard Newton method employed here follows the rather naive procedure to evaluate the material in every iteration, see Table **??**. In the highly nonlinear saturation phase, $0.03s < t \leq 0.06$, all methods require more Newton iterations per step and update the Jacobian almost at every time step. Bypassing element evaluations implies a linearity assumption and as a consequence the Newton iteration will require less Jacobian updates, Fig. **??**, but with the drawback of a larger error. After the saturation level is reached, $t > 0.06$, the field problem behaves again rather linearly and the updates of the simplified and bypassing Newton are clearly reduced.

The performance of this approach depends on the choice of the error norms, tolerances and device characteristics. We found the heuristic to be insensitive to changes in the parameters, especially for rather linear or fully saturated models, because the change in the saturation cause the high computational costs. For example in an induction machine, where the saturation rotates, we are forced to recompute the Schur complement more often, but the rotation is still determined by the energy and not by the frequency of a pulsed input. Especially in those applications one can further optimize the method and interpolate from previous Schur complements in dependence of the rotor angle and reuse them in the stationary phase.

When using an adaptive step-size control it should reflect that the recomputation of the inductance matrix $\mathbf{L}_h$ should be avoided if the step size h changes only insignificantly. On the other hand the application of an adaptive step size control

to problems with pulsed inputs as described here is not recommended due to high amounts of rejected steps. Thus a fixed step size is here typically no additional constraint.

7 Conclusion

Applying the Schur complement approach to MQS devices yields small element stamps that are equivalent to the constitutive relation of the series connection of inductors and resistors. The additional costs of the complement computation can be neglected if solvers with multiple right-hand side techniques are available. The presented heuristics to bypass Newton iterations reduce the computational costs clearly and they automatically detect when full Newton iterations are necessary. Due to bypassing, both problems are quasi decoupled and the time-integration of the circuit is cheapened because only basic elements are evaluated. This decoupling exploits the multirate time behavior of the coupled system if present.

Acknowledgements This work was partially supported by the EU within the ICESTARS project, by the German Academic Exchange Service "DAAD Jahresprogramm für Doktoranden" and the post-doc program of the "FG Mathematik and Informatik" of the Bergische Universität Wuppertal.

References

1. Vaananen, J.: Circuit theoretical approach to couple two-dimensional finite element with external circuit equations. IEEE Trans Magn **32**(2), 400 –410 (1996).
2. Feldmann, U., Miyake, M., Kajiwara, T., Miura-Mattausch, M.: On local handling of inner equations in compact models. In: Roos and Costa: Scientific Computing in Electrical Engineering SCEE 2008. Springer (2010), pp. 143–150
3. Schöps, S., Bartel, A., De Gersem, H., Günther, M.: DAE-index and convergence analysis of lumped electric circuits refined by 3-D MQS conductor models. In: Roos and Costa: Scientific Computing in Electrical Engineering SCEE 2008. Springer (2010), pp. 341 – 350.
4. De Gersem, H., Weiland, T.: Field-circuit coupling for time-harmonic models discretized by the finite integration technique. IEEE Trans Magn **40**(2), 1334 – 1337 (2004).
5. Feldmann, U., Günther, M.: CAD-based electric-circuit modeling in industry I: mathematical structure and index of network equations. Surv Math Ind **8**(2), 97 – 129 (1999)
6. Bartel, A., Baumanns, S., Schöps, S.: Structural analysis of electrical circuits including magnetoquasistatic devices. Submitted.
7. Hairer, E., Nørsett, S.P., Wanner, G.: Solving Ordinary Differential Equations II: Stiff and Differential-Algebraic Problems, 2 edn. Springer Series in Computational Mathematics. Springer, Berlin (1996)
8. Schöps, S., De Gersem, H., Bartel, A.: A cosimulation framework for multirate time-integration of field/circuit coupled problems. IEEE Trans Magn **46**(8), 3233 – 3236 (2010).
9. Wimmer, G., Steinmetz, T., Clemens, M.: Reuse, recycle, reduce (3r) – strategies for the calculation of transient magnetic fields. Appl Numer Math **59**(3-4), 830–844 (2008).
10. Clemens, M., Weiland, T.: Iterative methods for the solution of very large complex-symmetric linear systems in electrodynamics. In: CMCMM, vol. 2, pp. 1–7 (1996)
11. Schöps, S., De Gersem, H., Bartel, A.: Fitting lumped machine models on the fly. Submitted to Applied Numerical Mathematics.